International Journal of Chemical, Materials and Biomolecular Sciences
ISSN: 2415-6620
Vol:12, No:12, 2018

Waste-Based Surface Modification to Enhance Corrosion Resistance of Aluminium Bronze Alloy

Wilson Handoko, Farshid Pahlevani, Isha Singla, Himanish Kumar, Veena Sahajwalla

***Abstract*—**Aluminium bronze alloys are well known for their superior abrasion, tensile strength and non-magnetic properties, due to the co-presence of iron (Fe) and aluminium (Al) as alloying elements and have been commonly used in many industrial applications. However, continuous exposure to the marine environment will accelerate the risk of a tendency to Al bronze alloys parts failures. Although a higher level of corrosion resistance properties can be achieved by modifying its elemental composition, it will come at a price through the complex manufacturing process and increases the risk of reducing the ductility of Al bronze alloy. In this research, the use of ironmaking slag and waste plastic as the input source for surface modification of Al bronze alloy was implemented. Microstructural analysis conducted using polarised light microscopy and scanning electron microscopy (SEM) that is equipped with energy dispersive spectroscopy (EDS). An electrochemical corrosion test was carried out through Tafel polarisation method and calculation of protection efficiency against the base-material was determined. Results have indicated that uniform modified surface which is as the result of selective diffusion process, has enhanced corrosion resistance properties up to 12.67%. This approach has opened a new opportunity to access various industrial utilisations in commercial scale through minimising the dependency on natural resources by transforming waste sources into the protective coating in environmentally friendly and cost-effective ways.

***Keywords*—**Aluminium bronze, waste-based surface modification, Tafel polarisation, corrosion resistance.

I. Introduction

ALUMINIUM bronze alloys are a series of Cu-Al alloys with addition elemental composition of Fe, Ni and Mn that balanced the alloy composition. The usage of this type of alloy has been extensively increased annually, due to its excellent combination of both chemical (oxidation, corrosion) and mechanical (abrasive, tensile strength, hardness, weldability, non-magnetic) properties [1], [2]. These features have brought Al bronze alloy the primary choice for many demanding industrial applications such as ship propellers and petrochemical manufacturers [3]. Additionally, this Al bronze alloy consists of multiphase microstructures – face-centred cubic (fcc) α-phase, martensitic body-centered tetragonal (bct) β-phase and inter-metallic ϰ-phase, due to the distinctive percentage of alloying addition that transforms different phases during heat treatment and quenching processes [3], [4]. Since various Al bronze alloy applications are mainly involved and exposed to highly corrosive or seawater environment, the risk of parts failure is high. Corrosion resistance properties of Al bronze alloy can be improved through different complex manufacturing process, e.g. increasing the use of alloying elements (such as Ni) with different post heat treatment process [5], laser cladding to generate protective coating [6] and cold spraying treatment [7]. However, employing one of these methods will increase in production time, manufacturing cost and use of natural resource.

Millions tonnes of industrial waste slags disposed of in the landfill sites annually and will cause a severe resources depletion and deterioration in the living environment [8]. Global waste plastic has nearly reached 40 million tonnes in 2014 and this number is projected to increase around 4-6% every year [9]. Nevertheless, less than 20% was recycled and the remained waste plastic ended in the landfill as this waste was classified as non-recycled plastics (NRP) [10].

The objective of current research is to incorporate these two major issues and addresses a solution by modifying the surface properties of Al bronze alloy through selective diffusion process using waste as resources to enhance its corrosion resistance properties. This is not only reducing the dependency on natural resources, but also offers many positive impacts to the environment and production cost perspectives.

II. Experimental

A. Materials

Al bronze alloy with nominal chemical composition of 11.0Al, 4.0Fe, 1.5Ni, 0.5Mn and balanced in Cu (in wt.%) was utilised in this study. Ironmaking slag with compound composition of 38.5Fe_2O_3, 12.0SiO_3, 7.0MnO, 30.0CaO, 4.5Al_2O_3, 7.1MgO, 0.3Na_2O, 0.4P_2O_5 and 0.2Cr_2O_3 and complex mixture of plastic waste from automotive shredded residue (ASR) were used for surface modification formation on the Al bronze alloy sample.

B. Sample Preparation

Two samples were precisely cut from the 18.5mm-diameter Al bronze alloy bar to suit the requirements for all instruments (4.5mm x 4.5mm x 3.0mm) by using diamond blade in Struers Minitom with low speed rate at 150rpm. Next, grinded with SiC abrasive paper to 4,000 grit and polished up to 1 μm with

Wilson Handoko is PhD Candidate and Research Assistant in SMaRT Centre at UNSW Sydney, NSW 2052, Australia (phone: (+61) 425-958-088; e-mail: w.handoko@unsw.edu.au).

Farshid Pahlevani is Senior Research Fellow in SMaRT Centre at UNSW Sydney, NSW 2052, Australia (e-mail: f.pahlevani@unsw.edu.au).

Isha Singla is an exchange student from Department of Materials and Metallurgical Engineering, Punjab Engineering College, Chandigarh, India (e-mail: i.singla@student.unsw.edu.au).

Himanish Kumar is an exchange student from Department of Mechanical Engineering, Punjab Engineering College, Chandigarh, India (e-mail: himanish.kumar@student.unsw.edu.au).

Veena Sahajwalla is director of SMaRT Centre and Laureate Professor in UNSW Sydney, NSW 2052, Australia (e-mail: veena@unsw.edu.au).

diamond suspension, then both samples were rinsed by ethanol, cleaned by ultrasonic cleaner and dried. One sample was mixed with the slag and plastic wastes, heat treated to 900 ºC with dwelling time of 2h and air cooled to room temperature. To reveal the microstructures, the etching process was implemented by using 5% Nital solution for approximately half an hour.

C. Microstructural Investigation

Microstructures of Al bronze alloy specimens have been investigated by employing polarised light microscopy through Nikon Eclipse ME-600. High reconstruction of two- and three-dimensional images by 3D laser scanning confocal microscope (3D LSCM) were employed to provide valuable roughness quantitative data and to analyse the difference of topographical surface before and after surface modification through MultiFileAnalyzer software.

D. Electrochemical Test

An electrochemical measurement for corrosion resistance properties of Al bronze alloys has been conducted by Versatile Multipotentiostat VSP300 and all quantitative data were compiled by EC-Lab v11.10 software to generate Tafel polarization curves. This instrument is connected to three channels with different function, such as reference electrode from Saturated Calomel Electrode (SCE), auxiliary electrode from platinum (Pt) electrode and working electrode from Al bronze alloy sample. Electrolyte of 3.5 wt.% NaCl solution (pH=6.8) was prepared and filled into the corrosion flat cell kit at room temperature of 24±1ºC. Tested area of the sample was 1cm^2 in diameter unit, in open circuit potential (OCP) system, with obtained potential value ranges between in a wide (±250mV vs. OCP) and narrow (±250mV vs. OCP) at scan rate of 0.5mV/s. Each value of corrosion current density, i_{corr} was determined by extrapolation of linear portion from corrosion potential, E_{corr} at OCP stability after immersion for 2h in corrosive solution and later be used to determine protection efficiency, P_{EF} of modified surface.

III. Results and Discussion

A. Morphological Analysis

At microscale analysis by polarised light microscopy, the comparison of images of Figs. 1 and 2 exhibits different morphological microstructure cross section before and after surface modification through heat treatment process in etching condition. On the base-material, it is obvious to observe only α (bamboo-like shape in light colour) and β (diffused and distributed among α phase in dark colour) existed, whereas enrich Fe kappa – ϰ phase (flake shape in dark colour) appeared to be after waste-based surface modification by preferential diffusion of Fe and Al elements onto both co-presence phases – α and β. Although this will result in decrease of Fe rich in the main substrate on these co-presence phases and not on the modified surface, but overall volume fraction of α phase increased, while β phase decreased as the ϰ phase arose [11]. The modified surface consists of uniform α phase with existence of secondary phase – finely distributed ϰ phase.

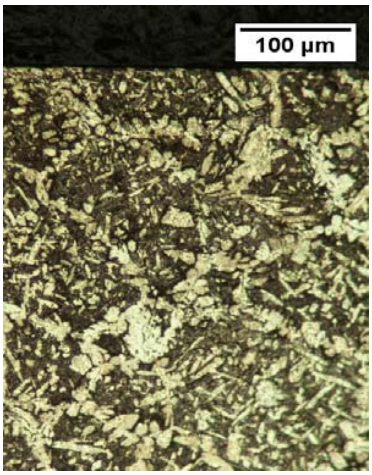

Fig. 1 Polarised light microscopy image of surface of Al bronze alloy before surface modification

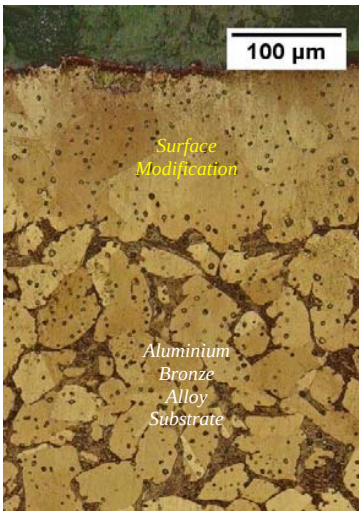

Fig. 2 Polarised light microscopy image of surface modification on Al bronze alloy after modified surface

This phenomenon occurred since the degradation of complex mixture of waste plastics at elevated temperature, which generated carbon monoxide (CO), carbon dioxide (CO_2) and methane (CH_4) gases and C-based by-product [11], [12]. These gases and C-based formations will reduce Fe_2O_3 and Al_2O_3 in the slag and transformed into Fe and Al atoms that can diffuse into surface of Al bronze alloy [12]. As result, these atoms diffused and bonded to aluminum bronze alloy substrate in the form of α and uniformly distributed fine ϰ phases [13].

After polarised light microscopy analysis, further microstructural investigation was performed by 3D LSCM in two- and three-dimensional images as shown in Figs. 3 and 4 for base-material and Figs. 5 and 6 for modified surface on Al bronze alloy sample respectively. Significant topographical difference before and after modified surface of Al bronze alloy

can be observed. Different size, shape, distribution and volume fraction of each α, β and ϰ phase can be accurately detected through the three-dimensional imaging. Additionally, α and β phases have changed their size and shape with α phase has become bulky grain and increase in volume fraction, while β phase has changed into packed shape with decrease numbers of its phase, and both phases became more Fe rich after promoting flake distributed ϰ phase. The presence of secondary phase after surface modification, this ϰ phase has the highest Fe content than both α and β phases combined [14].

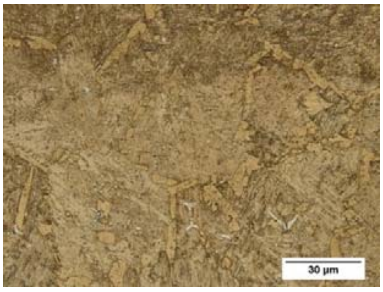

Fig. 3 Combination of optical and laser imaging of base-material Al bronze alloy in etching condition

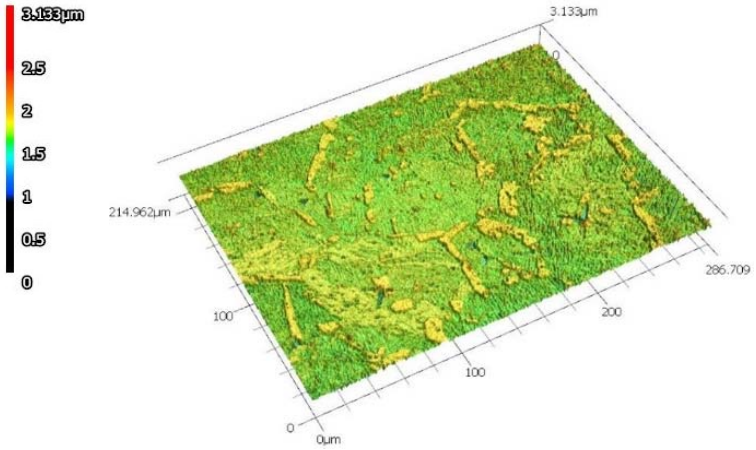

Fig. 4 Three-dimensional imaging of base-material Al bronze alloy in etching condition

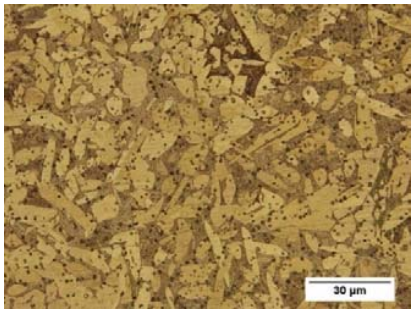

Fig. 5 Combination of optical and laser imaging of modified surface Al bronze alloy in etching condition

B. Potentiodynamic Measurements

A powerful tool for corrosion measurement through Tafel polarisation technique with immersion into 3.5 wt.% NaCl as the electrolyte for 2h was illustrated, to measure different corrosion rate on each sample. The cathodic branches (left hand side – charging) demonstrate the transformation reaction of hydrogen, while anodic branches (right hand side – discharging) indicate the metal dissolution reaction [15], [16]. Value of i_{corr} was drawn from extrapolating cathodic section line up to the point where vertically it passes through E_{corr}. In general, with lower i_{corr} and higher E_{corr} values, it reveals the improvement on corrosion resistance, thus promotes lower corrosion rate. Fig. 7 shows the comparison of Tafel polarisation curves on base-material and waste-based surface modification of Al bronze alloys.

The summary of each i_{corr} and E_{corr} values are presented in Table I. It can be elaborated that the lower value of i_{corr} at -2.15 mA/cm^2 with higher value of E_{corr} – approximately 18.09% towards noble side on the Al bronze alloy after modified its surface against the base-material. This is because of elemental compositions such as Al, Fe, Ni and Cu in the Al bronze alloy created protective modified surface – dominantly α and ϰ phases during the heat-treated process in oxygen condition that robustly diffused and bonded to the main substrate, performed higher-level of wear and corrosion resistance [17]. It can be stated that corrosion resistance properties after surface modification has been improved, and determination of protection efficiency of this protective surface can be implemented. Therefore, on the modified surface sample, the α has a primary role to protect the outer surface of Al bronze alloy as they became more Fe rich due to the enrich Fe from the slag that diffused and enhanced its Fe content in the phase. Thus, these bulky α phases will overlap the finely dispersed ϰ phases on both modified surface and main substrate in terms of corrosion resistance properties.

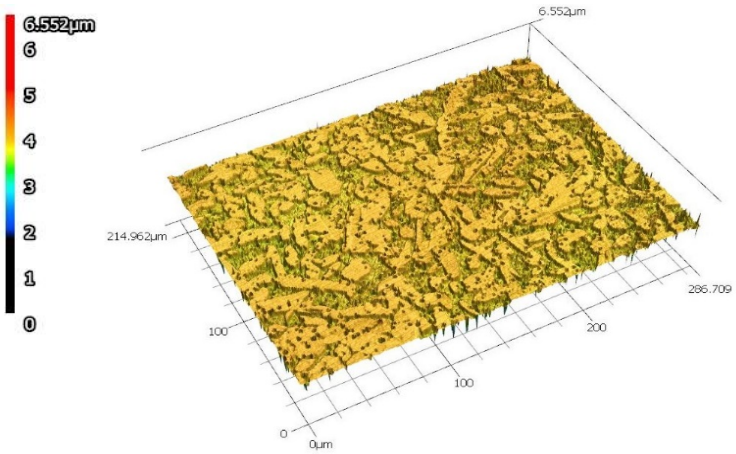

Fig. 6 Three-dimensional imaging of modified surface Al bronze alloy in etching condition

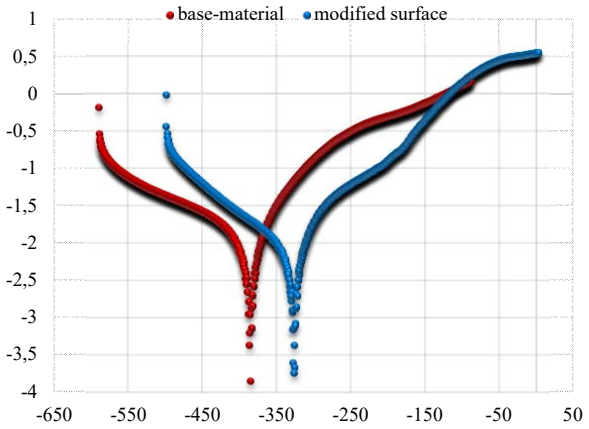

Fig. 7 Comparison of Tafel polarisation curves before and after surface modification on Al bronze alloy

TABLE I
THE COMPARISON OF ELECTROCHEMICAL QUANTITATIVE DATA BEFORE AND AFTER MODIFIED SURFACE CONDITION ON AL BRONZE ALLOY

Sample	Electrochemical Quantitative Data	
	i_{corr} (mA/cm^2)	E_{corr} (mV vs. SCE)
Base-Material	-1.85	-385
Modified Surface	-2.15	-326

C. Protective Efficiency Calculation

The protective efficiency of modified surface on Al bronze alloy can be calculated through obtained i_{corr} and E_{corr} values from Tafel polarisation curves. A standard Stern-Geary equation (1) [18] was used to evaluate the polarisation resistance, R_p value of each sample:

$$R_p = \frac{i_{corr} * b_a * b_c}{2.303 * (b_a + b_c)} \quad (1)$$

where b_a and b_c refer to the anodic and cathodic Tafel slopes ($\Delta E/\log i$), accordingly, then the percentage of protection efficiency, P_{EF} can be calculated using (2) [19]:

$$P_{EF} = \frac{R_p^{-1}(unmodified) - R_p^{-1}(modified\ surface)}{R_p^{-1}(modified\ surface)} * 100\% \quad (2)$$

The R_p and P_{EF} results of each Al bronze alloy specimens are presented in Table II. It is clearly demonstrated higher R_p on the waste-based surface modification Al bronze alloy sample that made contribution at 51.65kΩ.cm^2, whereas base-material accounted as 45.12 kΩ.cm^2. From these R_p values, the P_{EF} of modified surface of Al bronze alloy sample can be calculated and achieved around 12.67% protection efficiency for improving corrosion resistance properties. The main factor of enhancement in corrosion resistance properties is due to the presence of α phase with bulked and blocked grain size that is typically offer the best corrosion resistance than other phases [20], [21]. With the increase in grain size and shape in α phase after surface modification, the surface area contact will be less with other interface – β phase including inter-metallic ϰ phase, meaning that this will cause less boundary-to-boundary corrosion, thus reduction in corrosion rate [22], [23]. Therefore, the presence of secondary phase – ϰ phase has expanded the α phase grain size and shape on aluminum bronze alloy after heat treatment, as it became blocky Fe rich α phase with highly dense β phase that minimise the grain boundary corrosion, which has improved the corrosion resistance.

IV. CONCLUSION

This study has performed that corrosion rate values varied marginally between base-material and after modified surface on Al bronze alloy from waste sources through heat treatment. Microstructural and electrochemical corrosion properties have been investigated to analyse and determine the percentage of protective efficiency on the modified surface. Generating inter-metallic – ϰ phase as the part of surface modification on this grade of alloy, has improved the Fe content on both α and martensitic β phases with increasing volume percentage on α phase. After surface modification, these co-presence phases offered improvement in corrosion resistance in which α phase dominated as protective barrier that overlapped the presence

of ϰ phase on both modified surface and main substrate. With larger grain size of α phase, this will promote less surface area contact between other surrounding phases – β and ϰ phases. Enhancement of corrosion resistance properties after modified surface accounted for nearly 13% than base-material. The finding is crucial to produce Al bronze alloy parts with superior properties that will open a new opportunity to access different industrial applications through reducing the use of natural resources by converting waste sources into protective waste-based surface modification, which will lead to balance of both economic and environmental sustainability.

TABLE II
COMPARISON OF POLARISATION RESISTANCE AND PROTECTIVE EFFICIENCY FROM THE SURFACE MODIFICATION ON AL BRONZE ALLOY

Sample	Electrochemical Quantitative Data			
	b_a (mV/dec)	b_c (mV/dec)	R_p (kΩ.cm^2)	P_{EF} (%)
Base-Material	77.4	74.4	45.12	-
Modified-Surface	118.7	140.3	51.65	12.67

ACKNOWLEDGMENT

This research was supported under Australian Research Training Program (RTP) and Australian Research Council's Industrial Transformation Research Hub funding scheme (project IH130200025). We gratefully acknowledge the technical support provided by the Analytical Centre in the UNSW Sydney.

REFERENCES

[1] H. Krogstad and R. Johnsen. Corrosion properties of nickel-aluminium bronze in natural seawater—Effect of galvanic coupling to UNS S31603. *Corrosion Science*, 121, 2017, pp.43-56.
[2] W. Zhai, W. Lu, P. Zhang, M. Zhou, X. Liu and L. Zhou. Microstructure, mechanical and tribological properties of nickel-aluminium bronze alloys developed via gas-atomization and spark plasma sintering. *Materials Science and Engineering: A*, 707, 2017, pp.325-336.
[3] S. Neodo, D. Carugo, J. Wharton and K. Stokes, K. Electrochemical behaviour of nickel–aluminium bronze in chloride media: Influence of pH and benzotriazole. *Journal of Electroanalytical Chemistry*, 695, 2013, pp.38-46.
[4] A. Jahanafrooz, F. Hasan, G. Lorimer and N. Ridley. Microstructural development in complex nickel-aluminum bronzes. *Metallurgical Transactions A*, 14(10), 1983, pp.1951-1956.
[5] M. S. Rizi and A. H. Kokabi. Microstructure evolution and microhardness of friction stir welded cast aluminum bronze. *Journal of Materials Processing Technology*, 214(8), 2014, pp.1524-1529.
[6] M. Heydarzadeh Sohi, S. Hojjatzadeh, A. Khodayar and A. Amadeh. Liquid phase surface alloying of a nickel aluminum bronze alloy with titanium. *Surface and Coatings Technology*, 325, 2017, pp.617-626.
[7] H. Assadi, H. Kreye, F. Gärtner and T. Klassen. Cold spraying – A materials perspective. *Acta Materialia*, 116, 2016, pp.382-407.
[8] J. Wang, X. Huang, L. Wang, Q. Wang, Y. Yan, N. Zhao, D. Cui and Z. Feng. Kinetics study on the leaching of rare earth and aluminum from FCC catalyst waste slag using hydrochloric acid. *Hydrometallurgy*, 171, 2017, pp.312-319.
[9] N. J. Themelis, M. J. Castaldi, J. Bhatti, L. Arsova Energy and economic value of non-recycled plastics (NRP) and municipal solid wastes (MSW) that are currently landfilled in the fifty states Columbia University Earth Engineering Center, New York (2011).
[10] S. Anuar Sharuddin, F. Abnisa, W. Wan Daud and M. Aroua, M. Energy recovery from pyrolysis of plastic waste: Study on non-recycled plastics (NRP) data as the real measure of plastic waste. *Energy Conversion and Management*, 148, 2017, pp.925-934.
[11] P. Jain. Influence of Heat Treatment on Microstructure and Hardness of Nickel Aluminium Bronze (Cu-10Al-5Ni-5Fe). *IOSR Journal of Mechanical and Civil Engineering*, 4(6), 2013, pp.16-21.
[12] C. Zhang, P. Li and B. Cao. Decarboxylation crosslinking of polyimides with high CO_2/CH_4 separation performance and plasticization resistance. *Journal of Membrane Science*, 528, 2017, pp.206-216.
[13] V. Beura, V. Xavier, T. Venkateswaran and K. Kulkarni. Interdiffusion and microstructure evolution during brazing of austenitic martensitic stainless steel and aluminum-bronze with Ag-Cu-Zn based brazing filler material. *Journal of Alloys and Compounds*, 740, 2018, pp.852-862.
[14] J. Basumatary and R. J. K. Wood. Different methods of measuring synergy between cavitation erosion and corrosion for nickel aluminium bronze in 3.5% NaCl solution. *Tribology International*. (2017).
[15] C. Wang, C. Jiang, Z. Chai, M. Chen, L. Wang and V. Ji. Estimation of microstructure and corrosion properties of peened nickel aluminum bronze. *Surface and Coatings Technology*, 313, 2017, pp.136-142.
[16] W. Handoko, F. Pahlevani and V. Sahajwalla. The Effect of Low-Quantity Cr Addition on the Corrosion Behaviour of Dual-Phase High Carbon Steel. *Metals*, 8(4), 2018, pp. 199.
[17] F. Yang, H. Kang, E. Guo, R. Li, Z. Chen, Y. Zeng and T. Wang. The role of nickel in mechanical performance and corrosion behaviour of nickel-aluminium bronze in 3.5 wt.% NaCl solution. *Corrosion Science*, 139, 2018, pp.333-345.
[18] M. Stern and A. L. Geary. Electrochemical polarization I. A theoretical analysis of the shape of polarization curves. *Journal of The Electrochemical Society*, 104, 1957, pp. 55-63.
[19] J. Bockris and A. K. N. Reddy, A. *Modern Electrochemistry*. New York: Kluwer Academic Publishers (2000).
[20] Z. Qin, Q. Zhang, Q. Luo, Z. Wu, B. Shen, L. Liu and W. Hu. Microstructure design to improve the corrosion and cavitation corrosion resistance of a nickel-aluminum bronze. *Corrosion Science*, 139, 2018, pp.255-266.
[21] Y. Su, G. Liu, D. Wu and Z. Liu. The research of corrosion resistance of aluminum-bronze surfacing layer. *2nd International Conference on Electronic & Mechanical Engineering and Information Technology*, (2012).
[22] W. Handoko, F. Pahlevani and V. Sahajwalla. Corrosion Behaviour of Dual-Phase High Carbon Steel—Microstructure Influence. *Journal of Manufacturing and Materials Processing*, 1(2), 21, 2017.
[23] S. Thapliyal and D. K. Dwivedi. On cavitation erosion behavior of friction stir processed surface of cast nickel aluminium bronze. *Wear*, 2017, 376-377, pp.1030-1042.